NJC

Accepted Manuscript

This is an *Accepted Manuscript*, which has been through the Royal Society of Chemistry peer review process and has been accepted for publication.

Accepted Manuscripts are published online shortly after acceptance, before technical editing, formatting and proof reading. Using this free service, authors can make their results available to the community, in citable form, before we publish the edited article. We will replace this *Accepted Manuscript* with the edited and formatted *Advance Article* as soon as it is available.

You can find more information about *Accepted Manuscripts* in the Information for Authors.

Please note that technical editing may introduce minor changes to the text and/or graphics, which may alter content. The journal's standard Terms & Conditions and the Ethical guidelines still apply. In no event shall the Royal Society of Chemistry be held responsible for any errors or omissions in this *Accepted Manuscript* or any consequences arising from the use of any information it contains.

ROYAL SOCIETY OF CHEMISTRY

www.rsc.org/njc

G.A

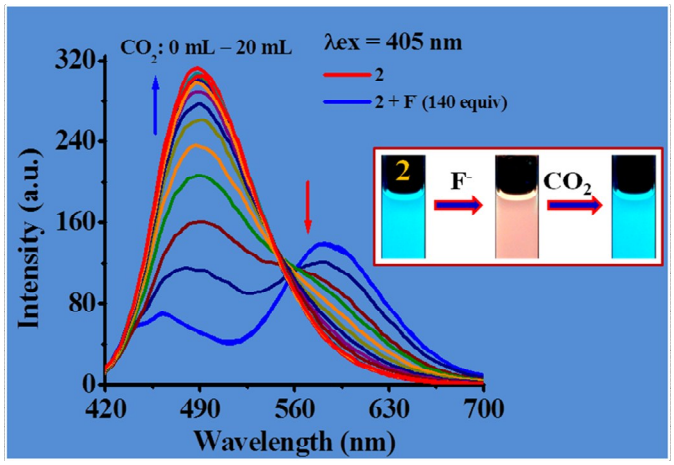

An Efficient ICT based Fluorescence Turn-On Dyad for Selective Detection of Fluoride and Carbon dioxide

Rashid Ali, Syed S. Razi, Ramesh C. Gupta, Sushil K. Dwivedi and Arvind Misra*

Department of Chemistry, Faculty of Science, Banaras Hindu University, Varanasi – 221 005 UP INDIA

arvindmisra2003@yahoo.com;amisra@bhu.ac.in

Abstract

A new intramolecular charge transfer (ICT) based fluorescence *turn-on* ratiometric probe **2** (*D–π—A* type) have been designed and synthesized by bridging imidazole (donor, *D*) and benzothiazole (acceptor, *A*) moieties through phenyl ring. The photophysical behavior of probe **2** in solvents of different polarity and at different pH has been investigated. Upon interaction with different class of anions probe **2** showed selective high affinity for fluoride anion (F^-) in aqueous DMSO (20%) solution. The ratiometric fluorescence turn-on behavior displayed by **2** with F^- is attributed to change in ICT process. Job's plot analysis revealed a 1:1 binding stoichiometry for **2**+F^- interactions with high binding constant and detection sensitivity (30 ppb). Moreover, a solution of **2**+F^- enabled detection of CO_2 (~100 ppb; 2.29 μM) through enhanced emission. The mode of interaction has been confirmed by ^{1}H NMR titration studies which suggested about the deprotonation of -*N*H fragment of imidazolyl unit in the presence of F^-.

Keywords: Chemosensor, ICT, F^- , CO_2

Introduction

Construction of good organic molecular scaffolds for recognition and sensing of anions with high sensitivity and selectivity is an interesting research area in the field of supramolecular chemistry.[1] Recently, great efforts have been made to develop biotic receptors for anionic species.[2-5] Among the various class of anions the recognition of fluoride anion (F^-) is of paramount importance due to its important roles in different biological, environmental and industrial processes.[3,4] Fluoride (F^-) is useful in dental care and in treatment of osteoporosis.[5] However, a high intake of fluoride from drinking water is believed to cause fluorosis, nephrotoxic changes urolithiasis in organism and even cancer.[6] Moreover, fluoride ions are also associated with the refinement of uranium used in the manufacture of nuclear weapons.[7] The Environmental Protection Agency (EPA, USA) has recommended 2 ppm permissible level of fluoride in water.[8] Thus the development of naked eye sensitive colorimetric and fluorogenic anion sensing systems has great implication in getting qualitative and quantitative information, and is challenging because of structural diversity and physical properties of different class of anions.[4-9]

In recent past considerable efforts have been made to detect fluoride using different chromophoric and fluoroionophore units such as, BODIPY, urea or thiourea, amide, phenol, cationic borane, silicon etc.[5] However, examples of a good sensing system which can detect F^- ions *via* intramolecular charge transfer (ICT) and ratiometric fluorescence response are limited in number.[10] Ratiometric fluorescent probe/sensors provide the practical advantage of built in corrections for environmental effects by allowing simultaneous detection at two signals.[11] Fluorescence based chemosensors, due to high sensitivity, simplicity and cost effectiveness are widely applicable in various areas such as, medicine, industry and the environment.[12]

Furthermore, the imidazole derivatives due to favorable properties such as, stability, high tuneable photophysical properties, extinction coefficient, and ease of synthesis enable the application of these chromophores in different areas.[13] Recently, a limited number of imidazole based systems have been exploited to develop OLED materials[14] and chemosensors.[15] A receptor system containing imidazole type ionophore is susceptible to detect anions either by H–bonding interaction or deprotonation of

potential –*N*H fragment.[3,16] Moreover, the typical structural change on donor and acceptor moieties and change in photophysical behavior due to a push-pull mechanism[17] may be easily followed by UV-vis, fluorescence and NMR studies.[18]

Additionally, carbon dioxide (CO_2) plays vital role in human physiology and has important diagnostic application in medical sciences.[19,20] On the other hand, CO_2 is an important green house gas which is a major factor for global climate change including critical global warming.[21] Thus, it is highly desirous to monitor and detect CO_2 sensitively in the environment. As well, quantification of CO_2 before its release into the atmosphere, in high CO_2 level containing anthropogenic gas streams (e.g., flue gas, syngas, biogas, etc.) is equally important.[21] Among various analytical methods, optical chemosensors for CO_2 have attracted considerable interest due to their simple, inexpensive and rapid sensing abilities.[19–24] Gunnlaugsson et al, earlier on suggested that anionic amine function, generated *in situ* by fluoride anion is a suitable substrate to react with CO_2.[22] Recently, Yoon et al, utilized benzobisimidazolium and bispyrene derivatives as a new class of CO_2 sensing probes, in which *in situ* generated carbene and anionic amide function displayed unique anion-activated CO_2 sensing mechanism through a simple colorimetric and fluorescent changes.[19,21]

Keeping these facts in mind our ongoing research is currently paying attention toward the development of some efficient fluorescent organic scaffolds/motifs to detect anions sensitively in different media.[25] Through this contribution we present a design and synthesis of a new class of intramolecular charge transfer (ICT) probe **2** and its potential application to recognize F^-. The objective of designing a selective and sensitive F^- responsive ratiometric probe has been achieved by developing a conjugated π-electron system containing specific ionophores, the –*N*H fragment, in which the electron rich imidazole (the donor) and electron deficient thiazole (as an acceptor) units are linked through a phenyl ring. As expected, probe **2** upon interaction with different anions has shown ratiometric fluorescence response toward F^- selectively, in aqueous-dimethylsulfoxide (20% solution). While the anion activated probe, **2**+F^- showed unique chromo and fluorogenic response to detect CO_2 with high sensitivity.

RESULTS AND DISCUSSION

Synthesis and Photophysical Behavior of Probe 2

The multi-component reactions (MCR) involving three or four different substrates has emerged as a powerful one-pot transformation strategy for the synthesis of chemically and biologically important organic frameworks.[26,27] The one-step synthesis of imidazole derivatives encouraged us to involve carbonyl compounds that may be further utilized to introduce other functionalities and extend the π-conjugation for better photophysical properties. Probe **2** was synthesized in two steps (Scheme 1). The synthesis of imidazole derivative **1a** and **1b** was carried out by one pot multi-component reaction[27] in which benzaldehyde and 4-formylbenzoic acid, benzil and NH_4OAc were refluxed in glacial acetic acid. Subsequently, compound **1b** was refluxed with 2-aminothiophenol in polyphosphoric acid (PPA) to get probe **2** in quantitative yield. The compounds were well characterized by ^1H NMR, ^{13}C NMR, IR and ESI-MS spectroscopy data (Figure S5-S8, Supporting Information).

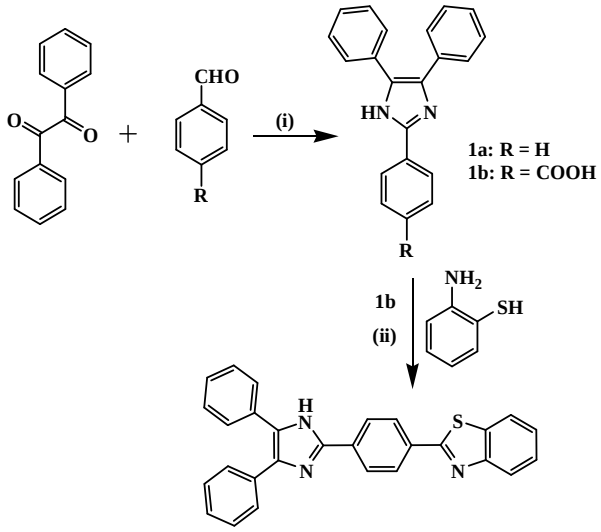

Scheme 1: (i) CH_3COONH_4/Glacial Acetic acid/110 ^0C (ii) PPA/Δ

The photophysical behavior of compound **2** (10 μM) was investigated in solvents of different polarity and data are summarized in Table–1. Probe **2** possess a typical *D-π-A* type structural motif and displayed different photophysical properties and good solvatochromism in the solvents (such as, hexane, 1,4-dioxane, chloroform

tetrahydrofuran, dimethylformamide, acetonitrile and dimethylsulfoxide) of different polarity.[28] (Figure–S9, Table 1). Moreover, in DMSO upon increasing the percentage of water (>30%) the intensity of probe decreased gradually along with change in color of solution (Figure S10). This is due to dominance of H-bonding interaction between fluoroionophore and water molecules as a result of decrease in extent of intermolecular charge transfer between the antibonding orbital of the –NH fragment of probe **2** and lone pair of electrons available in DMSO.[29] Therefore, the selectivity of probe **2** toward different class of anions has been studied in aqueous–DMSO (20% solution). The pH of the medium was found to be ~ 7.5.

Table 1: Photophysical properties of **2**

Entry	λ_{max} (nm)	Molar absorptivity $\varepsilon = M^{-1}cm^{-1}$	λ_{em} (nm)	Stoke's Shift $\Delta\bar{\upsilon}$ (cm^{-1})	Quantum yield Φ
Hexane	368 298	19,179 14,518	442	4550	0.39
Dioxane	367 294	18,197 13,289	458	5414	0.49
$CHCl_3$	369 301	16,851 12,509	461	5408	0.52
THF	371	18,530	466	5495	0.49
DMF	370 284	20,646 17,517	482	6280	0.44
ACN	357 296	19,087 13,772	484	7350	0.48
DMSO	370 302	20,082 16,086	488	6462	0.53
MeOH	356 296	20,215 15,325	490	7681	0.45

Anion selectivity of Probe 2

UV-vis spectrum of **2** (5μM) showed an intramolecular charge transfer (ICT) band at 370 nm ($\varepsilon = 1.90 \times 10^4\ M^{-1}\ cm^{-1}$) and a high energy band at 302 nm ($\varepsilon = 1.55 \times 10^4\ M^{-1}\ cm^{-1}$) in H_2O-DMSO (20%). Similarly, upon excitation at 370 nm probe **2** showed emission maxima at 488 nm (Φ_2 = 0.53). The affinity of probe **2** toward different class of anions (140 equiv) such as, F^-, Cl^-, Br^-, I^-, NO_3^-, N_3^-, SO_4^{2-}, $H_2PO_4^-$, CO_3^{2-}, AcO^-, CN^-, and SCN^- has been examined through absorption and emission spectroscopy. Notably, upon interaction with different anions probe **2** displayed high selectivity for F^- in which the ICT band disappeared completely and a new transition

band appeared at 455 nm (ε = 1.82 x 10^4 M^{-1} cm^{-1}) and naked-eye sensitive orange-red color appeared in the solution. Moreover, CN^- and AcO^- anions also showed affinity with probe, relatively less, in which molar absorbtivity at ICT band decreased around ~30-40% (Figure-1a).

Similarly, upon interaction with tested anions the fluorescence intensity of **2** (1µM, λ_{ex}=370 nm) centered, at 488 nm exhibited fluorescence quenching with AcO^- (~17%) and CN^- (~52%) anions. However, upon interaction with F^- the emission centered at, 488 nm diminished and a dual emission band appeared at 460 and 586 nm (Φ_{2+F^-} = 0.1) (Figure-1b). The intense blue color of solution, under UV light, switched–on immediately with F^- to a naked eye sensitive light pink color (Figure-2, images A). The interaction with other tested anions revealed insignificant change in the photophysical behavior of **2**. Further to ascertain high selectivity of **2** toward F^- a competitive anion interference studies have been performed by the addition of excess of tested anions (150 equiv.) to a probable solution of **2+F$^-$** and reversibly, by the addition of F^- to a solution of **2** containing another tested anions. Insignificant change in the absorption and emission spectrum of **2+F$^-$** suggested about the high selectivity of **2** for F^- (Inset of Figure 1a,b and Figure-2, images B).

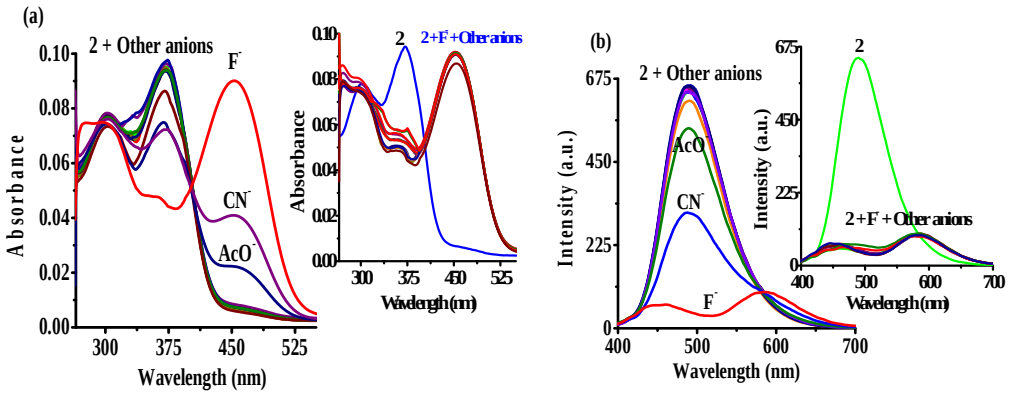

Figure 1: (a) Absorption (5µM) and (b) emission spectra of **2** (1µM) upon interaction with tested anions (140.0 equiv) in H_2O-DMSO (20%). Insets: Absorption and emission spectra of **2+ F$^-$** upon interference with competitive anions.

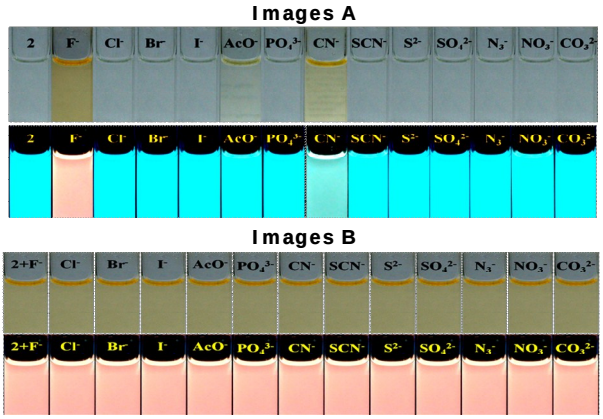

Figure 2: Chromogenic and fluorogenic response of **2** (10μM) upon interaction (Images A) and interference (Images B) with different anions (140.0 equiv) in H_2O-DMSO (20%; pH ~7.5).

Further, the binding affinity of **2** toward F^- has been realized through the absorption and emission titration experiments (Figure–3). Upon a gradual addition of F^- (0-140 equiv) to a solution of **2** the absorption spectra displayed ratiometric behavior in which band centered, at 370 nm decreased while the absorption of a new band at 455 nm enhanced concomitantly (Figure–3a). Similarly, the emission titration studies displayed ratiometric behavior in which fluorescence intensity of **2** (λ_{ex} 370 nm), centered at 488 nm diminished gradually and two new emission bands appeared at 455 nm and 586 nm (Figure–3b). The appearance of isosbestic and isoemissive points at 405 and 584 nm, respectively clearly supported about the existence of more than one species in the medium. Moreover, probe **2** upon excitation at isosbestic point, 405 nm displayed emission at 488 nm while upon titration with F^- (0-140 equiv) the intensity of a new emission band enhanced ratiometrically at 578 nm (Figure–3c). The observed significant red shift in the photophysical behavior of **2** upon interaction with F^- is attributed to enhance intramolecular charge transfer encounter due to deprotonation of –*N*H fragment.[18] The reaction stoichiometry between **2** and F^- has been realized by obtaining the absorption and emission spectra as a function of F^- concentration. The maxima at 0.5 mole fractions suggested about a 1:1 stoichiometry for a probe-fluoride interaction. For which, binding constant has been estimated through Benesi-Hildebrand (B-H) method[30] and were found to be K_{ass}(abs) = 1.01 x 10^4 /M and K_{ass}(em) = 1.28 x 10^4 /M respectively (Figure–3d and Figure S11b).

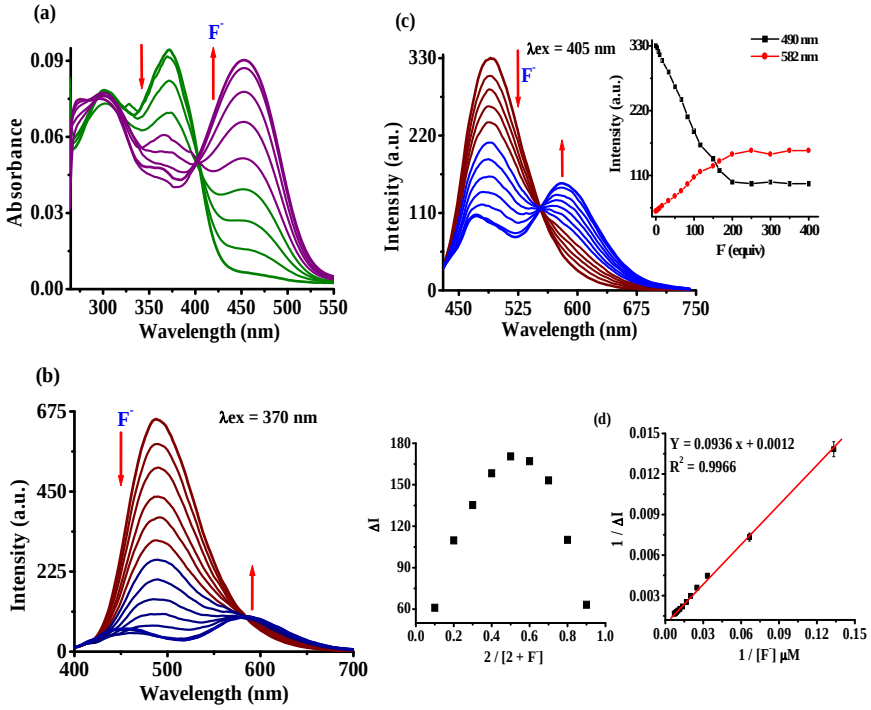

Figure 3: Absorption (5μM) (a) and emission (b) at λ_{ex} = 370 nm (c) at λ_{ex} = 405 nm titration spectra of **2** (1 μM) upon sequential addition of F^- (0 - 140.0 equiv.) in H_2O-DMSO (20%). (d) Job's plot and Benesi-Hildebrand plot based on emission spectra.

The limit of detection (LOD) of probe **2** for F^- has been estimated as reported previously.[31] An approximately straight line calibration curve, obtained by taking the emission spectra of **2** at different concentration (1.0 to 0.4 μM) suggested about a linear correlation between intensity and concentrations of the probe with standard deviation 0.6987 (Figure–S12a). Further, from the slope of the fluorescence curve, obtained between ΔI ($I - I_0$) (where I_0 and I illustrate the emission intensities of **2** in the presence and absence of F^-) and concentration of the anions in the aforementioned range, the calibration sensitivity (m) was estimated and was found to be 1.3228 (Figure–S12b). Now employing equation (3) the limit of detection (LOD) for F^- was calculated and was found to be 1.58 μM (30 ppb) which is well below the recommended level and comparable to other reported methods.[5]

pH Study of probe 2 in HEPES Buffer

The photophysical behavior displayed by **2** in the presence of F^- suggested about the deprotonation of –*N*H fragment of imidazolyl unit.[18] Consequently, the observed ratiometric enhanced emission is attributed to polarization and/or charge propagation of an increase electron density on the imidazolyl unit. Moreover, the moderately weak acidic –*N*H function of imidazole unit is susceptible to protonation and deprotonation under acidic and alkaline pH. Therefore, to rationalize the effect of F^-, pH dependent photophysical behavior of **2** was investigated in HEPES buffer (10 mM, pH 7.04; 20% aqueous DMSO).

The absorption spectrum of **2** (5 μM) showed electronic transition bands at 368 nm (ε = 1.82 x 10^4 $M^{-1}cm^{-1}$) with a shoulder at 305 nm (1.41 x 10^{-4} $M^{-1}cm^{-1}$) (Figure S13a). Similarly, upon excitation at 368 nm probe **2** showed intramolecular charge transfer emission band at 496 nm (Figure S13b). Notably, under acidic (pH 6 to 1) and alkaline (pH 10 to 14) conditions the molar absorptivity of **2** decreased wherein, the band centered, at 368 nm disappeared and a new transition band appeared at 354 nm (ε = 1.23 x 10^4 $M^{-1}cm^{-1}$; Blue-shift, ~14 nm) and 430 nm (ε = 1.15 x 10^4 $M^{-1}cm^{-1}$ Red-shift, ~62 nm) respectively (Figure 4a and S13a). The formation of isosbestic points at 360 and 396 nm in acidic and alkaline medium, respectively suggested about the existence of more than one species in the medium. Similarly, under acidic pH (< 6) the emission intensity of **2** centered at 496 nm (λ_{ex} = 368 nm) decreased with a blue shift of ~10 nm while under alkaline (>10) condition dual emission band appeared at 450 nm (blue shift ~46 nm) and 580 nm (red shift ~84 nm) (Figure 4b and S13b) and the color of solution become orange –red. Additionally, probe **2** upon excitation at isosbestic point, 396 nm displayed ratiometric behavior under alkaline pH (8-14) in which, intensity of **2** centred, at 496 nm decreased and concomitantly the relative fluorescence intensity of a new emission band (at, 586 nm) enhanced progressively (Figure 5). However, under acidic pH the intensity of **2** quenched gradually (Figure 5, inset). Thus, acid-alkali titration studies clearly supported about the protonation-deprotonation in the medium.

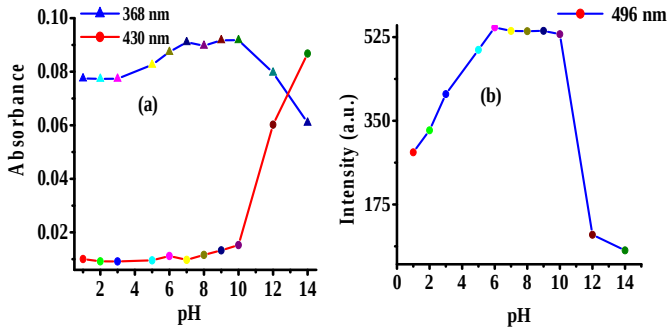

Figure 4: Change in (a) absorption and (b) emission (λ_{ex}=368 nm) intensity of **2** as a function of pH in HEPES buffer.

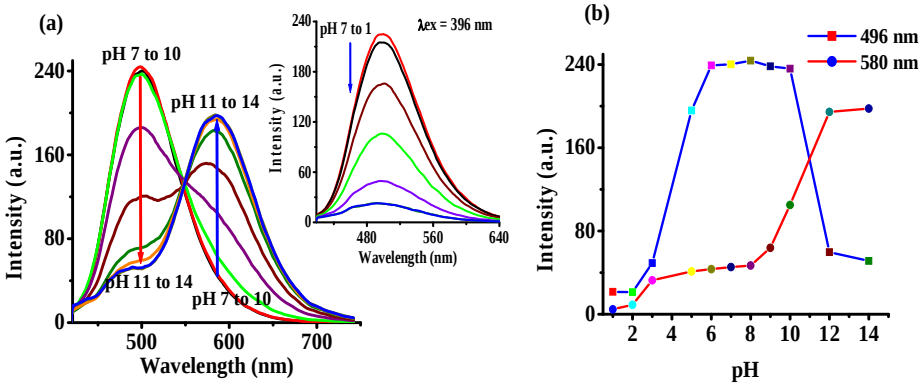

Figure 5: (a) Change in emission spectra of **2** (1μM) at different pHs in HEPES buffer, λ_{ex}=396 nm and (b) Change in emission intensity of **2** (1 μM) at 496 nm and 580 nm (λ_{ex}=396 nm) as a function of pH in HEPES buffer.

Nature of Interaction between 2 and F^-

To get deep insight about actual mechanism of interaction between **2** and F^- the ^{1}HNMR studies have been performed DMSO-d_6. ^{1}HNMR spectrum of **2** (2.1 x 10^{-2} M) (Figure–6, and S5) showed aromatic protons resonance in the range at δ 8.25-7.34 ppm. The imidazolyl –*N*H resonance appeared at δ 12.96(s) ppm due to hydrogen bonding interaction with solvent DMSO-d_6. Upon addition of F^- (0-2.0 equiv.) to a solution of **2** the -*N*H resonances broadened (Figure–S14, 15). Further addition of 3.0 to 5.0 equiv. of F^- the -*NH* resonances disappeared completely and the resonances of phenyl ring proton shifted upfield. A triplet appeared at δ 16.43 ppm suggested about

the formation of HF_2^- species[18] in the medium (Figure–S16, 17). Thus, the proton NMR studies clearly favored about the H-bonding interaction between –*N*H fragment of **2** and F^- followed by deprotonation. Consequently, the ICT increased due to charge propagation from imidazole to benzothiazole unit.

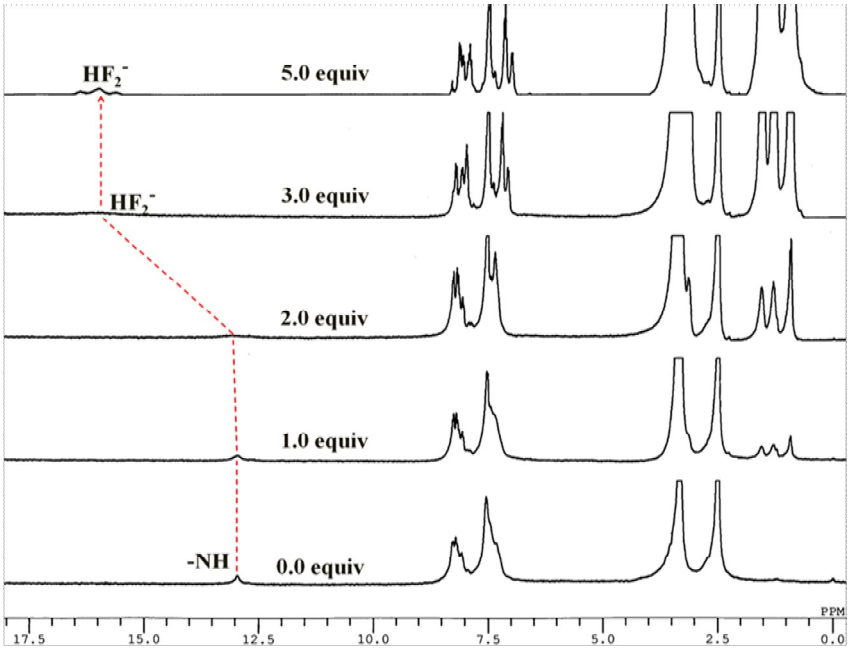

Figure 6: Stacked ^{1}H NMR spectra of **2** (2.1 x 10^{-2} M) upon addition of F^- ions (0-5.0 equiv) in DMSO-d_6.

DFT calculation:

The geometry optimization and quantum chemical calculations for **2** and the corresponding deprotonated product, **3** were performed by density functional theory (DFT) method as implemented in Gaussian 03 suits of program[32] employing basis set B3LYP/6-31G*. As shown in figure 7, the relevant occupied molecular orbital, HOMO (-0.30199 eV) is delocalized to the entire unit probe **2**, in which the electron density is spread over the imidazole-phenyl bridge-thiazole unit while unoccupied molecular orbital LUMO (-0.21798 eV) are distributed more towards thiazole –phenyl unit. Similarly, for **3** the HOMO (-0.29623 eV) is located to the entire unit while LUMO (-0.21833 eV) is more localized to thiazole-phenyl bridge. Thus, the molecular orbital approximation favors about the intramolecular charge transfer (ICT) from imidazole to thiazole unit. The deprotonation of imidazolyl –*N*H led to a further

polarization in electron density from the imidazole to thiazole unit. Furthermore, the energy gap between the HOMO and LUMO of **3** (ΔE = 0.0779 eV) was found less than that of probe **2** (ΔE = 0.08401 eV) and in good agreement with the red shift observed in the absorption spectra upon treatment with F^-. Thus both the theoretical and experimental observations corroborated the possible mode of interaction between **2** and fluoride anion.

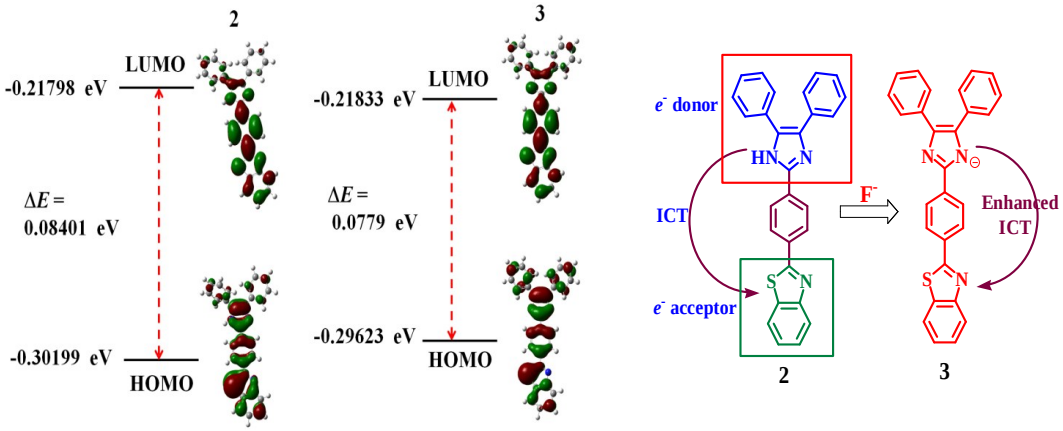

Figure 7: DFT optimized minimum energy structures and HOMO-LUMO energy difference between **2** and **3**. The proposed mechanism of interaction between probe **2** and F^- anion.

Analytical application of probe 2:

Detection of F^- on cellulose paper strips and silica coated slides

In order to make sure the potential applicability of probe **2** to detect fluoride anion on test paper strips and silica coated slides, small cellulose paper strips (Whatman^{TM}) containing different concentration of **2** (5, 2 and 1 mM) were prepared (1.5 × 2.0 cm^2) in acetone. The dried test paper strips were dipped in different concentration solutions of F^- (10×10^{-6}, 5×10^{-6}, and 1×10^{-6} M; of TBAF in ACN) for 5 min and then the air dried strips were visualised under UV light (at 365 nm). The visibility of color on the strip was good up to 1 mM level in which color of paper strips were changed from a light blue to ligth yellow (naked eye) and fluorescent blue to green (under UV light at 365 nm) (Figure 8a,b). The paper strip could able to detect F^- up to 10^{-7} M concentration. The paper strips of 0.1 and 0.01 mM concentration of probe could also able to detect F^- but the visibility of color on the strip was much better for 1.0 mM.

Similarly, the probe **2** was absorbed on silica coated slides and visualized under UV light (at 365 nm) before and after interaction with fluoride anion. The immediate naked-eye sensitive fluorescent color change from an off white to blue suggested the applicability of probe to sense anion on a solid surface (Figure 8c).

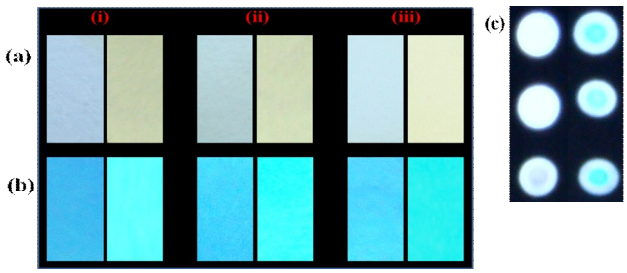

Figure 8: (a) Chromogenic (light blue to light yellow) and (b) fluorogenic (blue to green) response of **2** on paper strips containing different concentration of probe **2**; (i) 5 mM, (ii) 2 mM, (iii) 1 mM before and after addition of F^- (a) 10 x 10^{-6}, (b) 5.0 x 10^{-6} and (c) 1.0 x 10^{-6} M. (c) Fluorogenic response of **2** on Silica coated slides.

Anion induced CO_2 sensing:

The probe **2** contains an active –*N*H unit which can be utilized to detect CO_2 by a chemical-based optical method. This is because the deprotonation of acidic –*N*H function of chromophore by a suitable anion like, F^- generates negatively charged nitrogen, which act as an efficient nucleophile to react with CO_2. Therefore, in order to understand the potential applicability of probe an attempt has been made for anion induced CO_2 sensing and the change in typical photophysical behavior have been examined through the absorption and emission spectroscopy (Figure 9 and 10).

To investigate CO_2 sensing first, the solution of probe **2** was treated with TBAF to generate *in situ* an anion induced anionic probe, **2+F**$^-$. Upon passing the increasing volume of CO_2 to a solution of **2+F**$^-$ significant naked-eye sensitive color changes were observed in which the original color of probe revived. Similarly, the typical absorption band for **2+F**$^-$ centred, at 455 nm diminished with the revival of original absorption band of **2** (370 nm and 302 nm) along with formation of an isosbestic point at 404 nm (Figure 9). Moreover, the observed emission intensity of **2+F**$^-$ at 455 nm and 586 nm

(at λ_{ex} = 370 nm) upon bubbling increasing volume of CO_2 gas showed a gradual revival in emission intensity of **2** at 488 nm. Moreover, upon excitation at 405 nm, the emission intensity of **2+ F$^-$** centred, at 578 nm diminished ratiometrically on increasing the volume of CO_2 and original fluorescence intensity of **2** at 488 nm revived (Figure 10) with unique naked-eye sensitive colorimetric response wherein, the color of probe **2** changed from colorless to orange-yellow by F$^-$ revived to original color (Figure 9 images) while under UV light the reddish-orange color of **2+F$^-$** upon exposure with CO_2 regenerated actual intense blue color of **2** (Figure 10 images). Moreover, fluorescence titration data have been acquired to estimate the detection limit of **2+F$^-$** for CO_2 and was found to be 2.29 μM (~100 ppb) (Figure S18). Moreover, to understand high selectivity of probe for CO_2 the sensitivity of **2+F$^-$** has been investigated by passing other gases such as, H_2S, SO_2, and HCl (Figure S19). It is interesting to mention that upon interaction only in the presence of CO_2 the emission intensity of probe was revived while rest of the gases failed to exhibit any significant change in emission behavior of **2+F$^-$.**

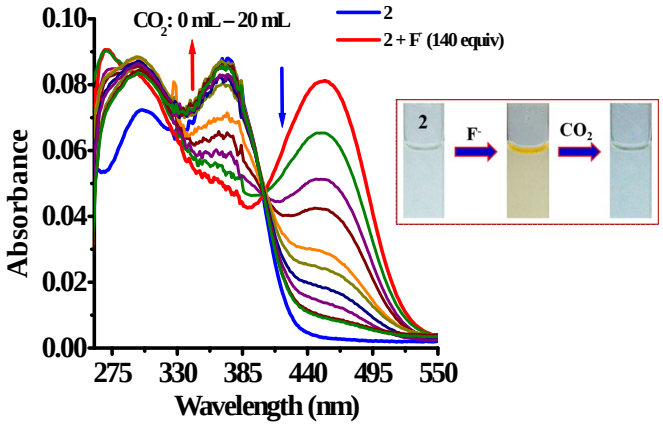

Figure 9: Change in absorption spectra of **2+** F$^-$ upon interaction with CO_2 in H_2O-DMSO (20%). Images: change in color of **2** with F$^-$ and CO_2.

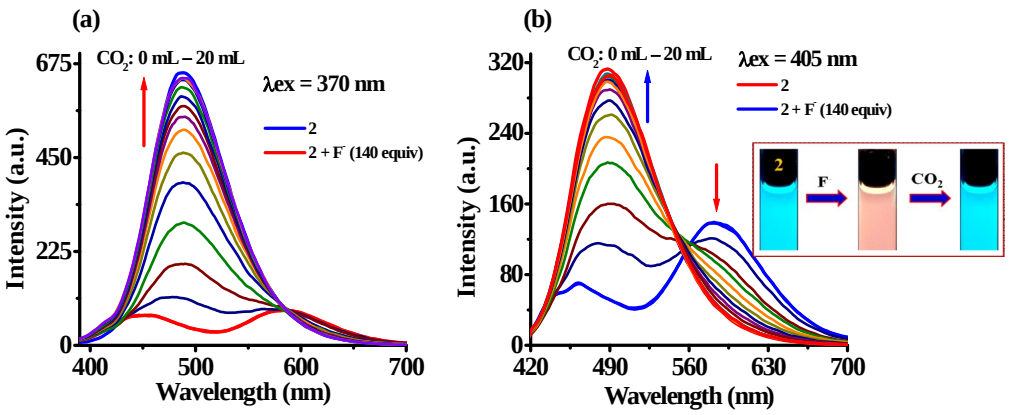

Figure 10: Change in emission spectra of **2** (1 μM) at (a) λ_{ex} = 370 nm (b) λ_{ex} = 405 nm, upon bubbling of different volume of CO_2 to the solution of **2**+ F^- in H_2O-DMSO (20%). Images: Showing respective color change of **2** with F^- and CO_2.

Further, the significant colorimetric response displayed by **2** in the presence and absence of fluoride anion and carbon dioxide is attributed to the formation of imidazolium hydrogen carbonate or imidazolium carbamic acid or its salt, generated from N-CO_2 adduct formed by the initial attack of negatively charged imidazolium ion to CO_2.[19,21] Carbamic acids are usually considered as highly unstable and upon formation they may typically release CO_2 to revive the corresponding free amine.[33a] Therefore to understand the actual mechanism of CO_2 sensing involved in the present case we acquired $^1H/^{13}C$NMR, FTIR and ESI-MS spectroscopic data of the probable imidazolyl N-CO_2 adducts, i.e. imidazolyl carbamic acid, **3** after passing the excess of CO_2 to a solution of **2** (35 mg; 0.08 mmol) and TBAF (2.0 equiv) in acetonitrile.

The ^1H NMR spectra showed a broad resonance at δ 13.01 ppm due to the partially deprotonated –*N*H function of imidazole unit of probe. However, the resonances appeared at δ 12.68 and δ 5.072 ppm may be assigned to the formation of imidazolyl carbamic acid[33b] (–NCOOH) (Figure-S20). Similarly, the resonances appeared at δ 183.3 and δ 163.883 ppm in ^{13}C NMR spectrum are assignable to the carbonyl carbon (C=O) of carboxylic acid and imidazolyl-N-carbamate anion (Figure-S21). Moreover, FTIR spectrum of probable adduct showed resonances at 1703 and 3208-2873 cm^{-1} due to the C=O and O-H stretching vibration of carboxylic function. The stretching

vibration bands at 3379 and 2341 cm^{-1} may be assigned to –NH and CO_2 respectively[33c] (Figure-S22). Thus, the spectroscopy studies suggested about the formation of adduct as well as about the existence of H-bonding interaction in the medium in between imidazolium N-CO_2 adduct and imidazolyl –*N*H unit of second molecule as shown in scheme-2. Nevertheless, the species formed in the medium are not very much stable[33a] we attempted to acquire the mass spectrum of adduct **3** to justify our hypothesis. Interestingly, the molecular ion peak corresponding to $[2+H]^+$ appeared at m/z 430.1354. However we could not observe any sharp signal corresponding to formation of imidazolium carbamate or carbonate salt probably due to poor stability of the adduct. However, a very weak molecular ion peak appeared at m/z 475.1361 $[2+CO_2+2H]^+$ corresponds to the formation of imidazolyl carbamic acid in the medium (Figure-S23). Based on above finding we proposed a plausible mechanism of CO_2 interaction has been shown in scheme-2.

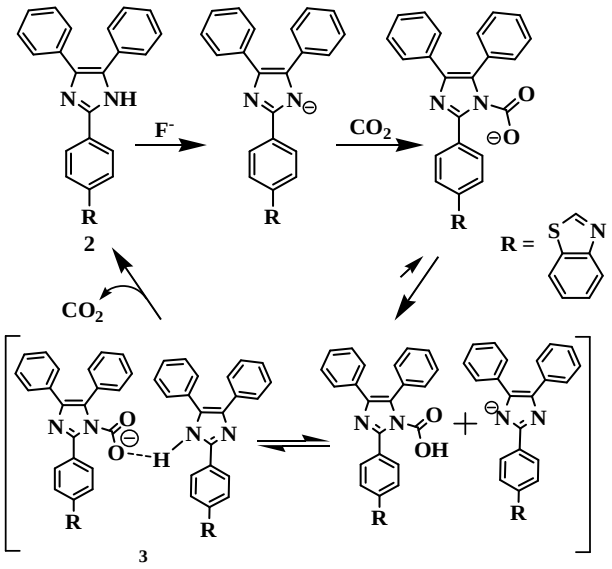

Scheme 2: A plausible mechanism of CO_2 interaction with probe.

Conclusion

In summary, an efficient donor-acceptor type intramolecular charge transfer (ICT) probe has been developed. The photophysical behavior of the probe has been examined in the solvents of different polarity. The anion interaction studies showed

that probe can be utilized as a potential chemosensor to detect F^- selectively and sensitively with naked-eye visual color changes in partial aqueous medium. Moreover, probe **2** has been utilized to detect CO_2 by a chemical-based optical method. The in situ generated anionic species, **2+F**$^-$ displayed unique colorimetric response along with revival in the typical photophysical properties of probe **2.** The proton NMR studies unequivocally supported about the deprotonation of moderately acidic imidazolyl –*N*H fragment in the presence of F^- anion and corroborated the observed changes in the photophysical behavior of probe, consequently.

Experimental

Synthesis of compound 1a and 1b: Benzil (1.05 g, 5 mmol), benzaldehyde or 4-formylbenzoic acid (5 mmol) and ammonium acetate (1.156 g, 15 mmol) were refluxed in glacial acetic acid (20 ml) for 4hr. After completion of reaction (monitored on TLC) the reaction mixture was cooled down to room temperature and poured into ice-water (20 ml). The precipitate so obtained was filtered, washed with cold water, and dried in air to obtain compound **1a** and **1b.**

1a. Yield, 1.26g (85%): ^{1}H NMR (300 MHz, DMSO-d_6)**:** δ (ppm): 12.58 (s, 1H, -NH), 7.52-7.23 (m, 15H, Ar); FT-IR (KBr) ν_{max} (cm^{-1}); 3329, 1588, 1516, 1495, 1435, 1381, 1336, 1272, 1168, 1146, 1107, 1076, 883, 764, 698.

1b.Yield, 1.2g (70%). ^{1}H NMR (300 MHz, DMSO-d_6)**:** δ (ppm): 12.90 (s, 1H, -NH), 8.20-8.17 (d, 2H, J = 7.5 Hz), 8.03 (s, 2H) 7.52-7.30 (m, 10H); IR (KB r) ν_{max} (cm^{-1}); 3415, 2924, 1650, 1621, 1614, 1517, 1427, 1370, 1318, 1242, 1158, 1105, 1062, 896, 781.

Synthesis of compound 2: Compound **1b** (170mg, 0.5 mmol) and 2-aminothiophenol (62.5mg, 0.5mmol) were refluxed for 16 hr in the presence of PPA (0.5g). After completion of reaction (monitored on TLC) the reaction mixture was quenched with water and resulting precipitate was washed with saturated solution of sodium hydrogen carbonate comprehensively to afford compound **2**. Yield 275 mg (64%). ^{1}H NMR (300 MHz, DMSO-d_6) δ (ppm): 13.0 (s, 1H, -NH),8.31-8.28 (d, 2H, J = 7.5 Hz), 8.22-8.19 (d, 2H, J = 8.4 Hz), 8.09-8.07 (d, 2H, J = 7.8 Hz), 7.57-7.47 (m, 12H). ^{13}C NMR (75MHz, DMSO-d_6) δ (ppm): 166.80, 153.61, 144.56, 134.47, 132.16,

129.40, 128.65, 127.65, 127.21, 126.72, 125.82, 125.55, 124.49, 122.83, 122.38; FT-IR (KBr) ν_{max} (cm^{-1}); 3370, 3055, 1586, 1601, 1479, 1432,1388, 1251, 1227, 1181, 1125, 1071, 966, 915, 842, 758, 727, 695. ESI-MS m/z: $[2 + H]^+$ for C28H19N3S, 430.2.

Acknowledgment

Authors are thankful to the Council of Scientific and Industrial Research (CSIR) (02(0199/14/EMR-II) and UGC New Delhi for financial assistance and fellowships (RA, SSR, RCG and SKD).

Supplementary data: General experimental detail, ^1H, ^{13}C NMR, FTIR, and ESI-MS.

References

1. (a) F. P. Schmidtchen and M. Berger, *Chem. Rev.*, 1997, **97**, 1609–1646; (b) X. Lou, D. Ou, Q. Li and Z. Li, *Chem. Commun.*, 2012, **48**, 8462-8477.

2. (a) M. Cametti and K. Rissanen, *Chem. Commun.*, 2009, 2809-2829; (b) S. Y. Kim and Hong, J.-I., *Org. Lett.*, 2007, **9**, 3109-3112.

3. M. Cametti and K. Rissanenb, *Chem. Soc. Rev*., 2013, **42**, 2016-2038.

4. (a) R.J. Carton, *Fluoride*, 2006, **39**, 163-172; (b) R. Hu, J. Feng, D. Hu, S. Wang, S. Li, Y. Li and G. Yang, *Angew. Chem. Int. Ed*., 2010, **49**, 4915-4918.

5. (a) Y. Zhou, J. F. Zhang and J. Yoon, *Chem. Rev.*, 2014, **114**, 5511-5571; (b) S. Goswami, A. K. Das, A. Manna, A. K. Maity, H.-K. Func, C. K. Quah and P. Saha, *Tetrahedron Letters*, 2014, **55**, 2633-2638.

6. A. Wiseman, Handbook of Experimental Pharmacology, 20, *Springer-Verlag*, Berlin, 1970, pp. 48-97.

7. T. W. Hudnall, C.-W. Chiu and F. P. Gabbai, *Acc. Chem. Res*., 2009, **42,** 388-397.

8. J.-A. Gu, V. Mania and S.-T. Huang, *Analyst*, 2015, **140**, 346-352.

9. R. Martinez-Manez and F. Sancenon, *Chem. Rev.*, 2003, **103**, 4419-4476.

10. (a) A. Aydogan, D. J. Coady, V. M. Lynch, A. Akar, M. Marquez, C. W. Bielawski and J. L. Sessler, *Chem. Commun*., 2008, 1455-1457; (b) C. Bhaumik, D. Saha, S. Das and S. Baitalik, *Inorg. Chem*., 2011, **50**, 12586-125600; (c) D. Maity, S. Das, S. Mardanya and S. Baitalik, *Inorg. Chem*., 2013, **52**, 6820-6838; (d) N. Kumari, S. Jha and S. Bhattacharya, *J. Org. Chem.*, 2011, **76**, 8215-8222; (e) Z. Guo, N. R. Song, J. H. Moon, M. Kim, E. J. Jun, J. Choi, J. Y. Lee, C. W. Bielawski, J. L. Sessler and J. Yoon, *J. Am. Chem. Soc.*, 2012, **134**, 17846-17849.

11. (a) D. Srikun, E. W. Miller, D. W. Domaille, J. Christopher and C. J. Chang, *J. Am. Chem. Soc.*, 2008, **130**, 4596-4597; (b) H. Yu, Q. Zhao, Z. Jiang, J. Qin and Z. Li, *Sensors and Actuators B*, 2010, **148**, 110-116.

12. J. R. Lakowicz, ‘‘*Principles of Fluorescence Spectroscopy*’’, 3rd edition, Springer, New York 2006.

13. D. Burtscher, R. Saf and C. Slugovc, *J. Polym. Sci., Part A: Polym.Chem.*, 2006, **44**, 6136-6145.

14. (a) K. Benelhadj, J. Massue, P. Retailleau, G. Ulrich and R. Ziessel, *Org. Lett.*, 2013, **15**, 2918–2921; (b) X. Zhang, J. Lin, X. Ouyang, Y. Liu, X. Liu and Z. J. Ge, *Photochem. Photobiol.*, 2013, **268**, 37– 43.

15. (a) K. Zheng, W. Lin and L. Tan, *Org. Biomol. Chem.*, 2012, **10**, 9683-9688; (b) K. C. Song, H. Kim, K. M. Lee, Y. S. Lee, Y. Do and M. H. Lee, *Sens Actuators B.*, 2013, **176**, 850-857.

16. (a) A. P. de Silva, H. Q. N. Gunaratne, T. Gunnlaugsson, A. J. M. Huxley, C. P. McCoy, J. D. Rademacher and T. E. Rice, *Chem. Rev.*, 1997, **97**, 1515-1566; (b) J. L. Sessler, S. Camiolo and P. A. Gale, *Coord. Chem. Rev.*, 2003, **240**, 17-55; (c) K. Choi and A. D. Hamilton, *Coord. Chem. Rev.*, 2003, **240**, 101-110; (d) K. M. K. Swamy, Y. J. Lee, H. N. Lee, J. Chun, Y. Kim, S-J. Kim and J. Yoon, *J. Org. Chem.*, 2006, **71**, 8626-8628; (e) X. Y. Liu, D. R. Bai and S. Wang, *Angew. Chem. Int. Ed.*, 2006, **45**, 5475-5478.

17. (a) P.A. Gale, *Coordination Chemistry Reviews*, 2003, **240,** 191-221; (b) R. M. Duke, E. B. Veale, F. M. Pfeffer, P. E. Krugerc and T. Gunnlaugsson, *Chem. Soc. Rev.*, 2010, **39**, 3936-3953; (c) J. V. Ros-Lis, R. Martínez-Máñez, F. Sancenón, J. Soto, K. Rurack and H. Weißhoff, *Eur. J. Org. Chem.*, 2007, 2449–2458; (d) C. Marín-Hernandez, L. E. Santos-Figueroa, M. E. Moragues, M. M. M. Raposo, R. M. F. Batista, S. P. G. Costa, T. Pardo, R. Martínez-Mañez and F. Sancenón, *J. Org. Chem.*, 2014, **79**, 10752-10761.

18. (a) P. Dydio, D. Lichosyt, J. Jurczak, *Chem. Soc. Rev.*, 2011, **40**, 2971-2985; (b) M. Shahid, P. Srivastava and A. Misra, *New J. Chem.*, 2011, **35**, 1690-1700; (c) A. Misra, M. Shahid and P. Dwivedi, *Talanta.*, 2009, **80**, 532-538; (d) A. Misra, M. Shahid and P. Srivastava, *Sensors and Actuators B*, 2012, **169**, 327– 340.

19. M. Lee, S. Jo, D. Lee, Z. Xu and J. Yoon, *Dyes and Pigments*, 2015, **120**, 288-292.

20. M. Lee, J. H. Moon, K. M. K. Swamy, Y. Jeong, G. Kim, J. Choi, J. Y. Lee and J. Yoon, *Sensors and Actuators B*, 2014, **199**, 369–376.

21. Z. Guo, N. R. Song, J. H. Moon, M. Kim, E. J. Jun, J. Choi, J. Y. Lee, C. W. Bielawski, J. L. Sessler and J. Yoon, *J. Am. Chem. Soc.*, 2012, **134**, 17846-17849.

22. T. Gunnlaugsson, P. E. Kruger, P. Jensen, F. M. Pfeffer and G. M. Hussey, *Tetrahedron Letters*, 2003, **44**, 8909-8913.

23. (a) X. Xie, M. Pawlak, M. Tercier-Waeber and E. Bakker, *Anal. Chem.*, 2012, **84**, 3163-3169; (b) Y. Liu, Y. Tang, N. N. Barashkov, I. S. Irgibaeva, J. W. Y. Lam, R. Hu, D. Birimzhanova, Y. Yu and B. Z. Tang, *J. Am. Chem. Soc.*, 2010, **132,** 13951-13953; (c) R. N. Dansby-Sparks, J. Jin, S. J. Mechery, U. Sampathkumaran, T. W. Owen, B. D. Yu, K. Goswami, K. Hong, J. Grant and Z.-L. Xue, *Anal. Chem.*, 2010, **82**, 593-600; (d) M. Ishida, P. Kim, J. Choi, J. Yoon, D. Kim and J. L. Sessler, *Chem. Commun*., 2013, **49**, 6950-6952.

24. (a) R. Ali, T. Lang, S. M. Saler, R. J. Meier and O. S. Wolfbeis, *Anal. Chem*., 2011, **83,** 2846-2851; (b) D. Wencel, J. P. Moore, N. Stevernson and C. McDonagh, *Anal. Bioanal. Chem.*, 2010, **398**, 1899-1907; (c) Q. Xu, S. Lee, Y. Cho, M. H. Kim, J. Bouffard and J. Yoon, *J. Am. Chem. Soc.*, 2013, **135**, 17751-17754; (d) X. Zhang, S. Lee, Y. Liu, M. Lee, J. Yin, J. L. Sessler and J. Yoon, *Sci. Rep.*, 2014, **4**, http://dx.doi.org/10.1038/srep04593.

25. (a) S. S. Razi, R. Ali, P. Srivastava and A. Misra, *Tetrahedron Letters*, 2014, **55**, 1052-1056; (b) S. S. Razi, R. Ali, P. Srivastava and A. Misra, *Tetrahedron Letters*, 2014, **55**, 2936-2941; (c) S. S. Razi, R. Ali, P. Srivastava, M. Shahid and A. Misra, *RSC Adv*., 2014, **4**, 22308-22317; (d) S. S. Razi, P. Srivastava, R. Ali, R. C. Gupta, S. K. Dwivedi, A. Misra, *Sensors and Actuators B*, 2015, **209**, 162-171.

26. (a) D. M. D'Souza, A. Kiel, D. P. Herten, F. Rominger and T. J. J. Muller, *Chem. Eur. J*. 2008, **14**, 529-547; (b) J. E. Biggs-Houck, A. Younai and J. T. Shaw, *Current Opinion in Chemical Biology*, 2010, **14**, 371-382; (c) B. B. Toure and D. G. Hall, *Chem. Rev.*, 2009, **109,** 4439-4486.

27. S. Park, J. E. Kwon, S .H. Kim, J. Seo, K. Chung, S.-Y. Park, D.-J. Jang, B. M. Medina, J. Gierschner and S. Y. Park, *J. Am. Chem. Soc.*, 2009, **131**, 14043-14049.

28. Y. Zhang, D. Li, Y. Li and J. Yu, *Chem. Sci.*, 2014, **5**, 2710-2716.

29. A. Misra and M. Shahid, *J. Phys. Chem. C*, 2010, **114**, 16726-16739.

30. H. A. Benesi and J. H. Hildebrand, *J. Am. Chem. Soc*., 1949, **71**, 2703-2707.

31. A. Misra, P. Srivastava and M. Shahid, *Analyst*, 2012, **137**, 3470-3478.

32. M. J. Frisch, G. W. Truncks and H. B. Schlegel, *GAUSSIAN 03, Revision E.01;Gaussian: Wallingford, CT* 2007.

33. (a) E. M. Hampe and D. M. Rudkevich, *Chem. Commun.*, 2002, 1450-1451; (b) G. A. Olah, T. Heiner, G. Rasul, and G. K. Surya Prakash, *J. Org. Chem.*, 1998, **63**, 7993-7998; (c) R.K. Khanna and M.H. Moore, *Spectrochimica Acta Part A*, 1999, **55**, 961-967.

Figure captions

Scheme 1: (i) CH_3COONH_4/Glacial Acetic acid/110 ^{0}C (ii) PPA/Δ

Table 1: Photophysical properties of **2**

Figure 1: (a) Absorption (5μM) and (b) emission spectra of **2** (1μM) upon interaction with tested anions (140.0 equiv) in H_2O-DMSO (20%). Insets: Absorption and emission spectra of **2+ F$^-$** upon interference with competitive anions.

Figure 2: Chromogenic and fluorogenic response of **2** (10μM) upon interaction (Images A) and interference (Images B) with different anions (140.0 equiv) in H_2O-DMSO (20%).

Figure 3: Absorption (5μM) (a) and emission (b) at λ_{ex} = 370 nm (c) at λ_{ex} = 405 nm titration spectra of **2** (1 μM) upon sequential addition of F$^-$ (0 - 140.0 equiv.) in H_2O-DMSO (20%). (d) Job's plot and Benesi-Hildebrand plot based on emission spectra.

Figure 4: Change in (a) absorption and (b) emission (λ_{ex}=368 nm) intensity of **2** as a function of pH in HEPES buffer.

Figure 5: (a) Change in emission spectra of **2** (1μM) at different pHs in HEPES buffer, λ_{ex}=396 nm and (b) Change in emission intensity of **2** (1 μM) at 496 nm and 580 nm (λ_{ex}=396 nm) as a function of pH in HEPES buffer.

Figure 6: Stacked ^{1}H NMR spectra of **2** (2.1 x 10^{-2} M) upon addition of F$^-$ ions (0-5.0 equiv) in DMSO-d_6.

Figure 7: DFT optimized minimum energy structures and HOMO-LUMO energy difference between **2** and **3**. The proposed mechanism of interaction between probe **2** and F$^-$ anion.

Figure 8: (a) Chromogenic (light blue to light yellow) and (b) fluorogenic (blue to green) response of **2** on paper strips containing different concentration of probe **2**; (i) 5 mM, (ii) 2 mM, (iii) 1 mM before and after addition of F$^-$ (a) 10 x 10^{-6}, (b) 5.0 x 10^{-6} and (c) 1.0 x 10^{-6} M. (c) Fluorogenic response of **2** on Silica coated slides.

Figure 9: Change in absorption spectra of **2+** F^- upon interaction with CO_2 in H_2O-DMSO (20%). Images: change in color of **2** with F^- and CO_2.

Figure 10: Change in emission spectra of 2 (1 μM) at (a) λ_{ex} = 370 nm (b) λ_{ex} = 405 nm, upon bubbling of different volume of CO_2 to the solution of 2+ F^- in H_2O-DMSO (20%). Images: Showing respective color change of 2 with F^- and CO_2.

Scheme 2: A plausible mechanism of CO_2 interaction with probe.